Separation and determination of degradation products of acid orange 7 by capillary electrophoresis/capacitively coupled contactless conductivity detector

Xin Wang [a], Ya Xiong [a,d,*], Tianyao Xie [b], Virender K. Sharma [c], Yuting Tu [a], Jiannan Yang [a], Shuanghong Tian [a], Chun He [a,d,*]

[a] School of Environmental Science and Engineering, Sun Yat-sen University, Guangzhou 510275, China
[b] School of Chemistry and Chemical Engineering, Sun Yat-sen University, Guangzhou 510275, China
[c] Chemistry Department, Florida Institute of Technology, 150 West University Boulevard, FL 32901, USA
[d] Guangdong Provincial Key Laboratory of Environmental Pollution Control and Remediation Technology, Guangzhou 510275, China

ARTICLE INFO

ABSTRACT

Capillary electrophoresis (CE) with capacitively coupled contactless conductivity detector (C^4D) was developed to separate azo-dyestuff acid orange 7 (AO7) and its six degradation products. The analyzed products were sulfamic acid, oxalic acid, benzenesulfonic acid, 4-hydroxybenzene sulfonic acid, phthalic acid, and 4-aminobenzene sulfonic acid. In developing the method, types and concentrations of running buffers, injecting voltage and time, and applied voltage were tested to obtain optimum conditions to analyze target compounds. The separation was successfully achieved within 10 min using a fused-silica capillary under the following conditions: 20 mmol L^{-1} acetate acid buffer, electrokinetic injection of -12 kV $\times$ 10 s, and applied voltage of -13 kV. The developed method was applied to analyze degradation products *in situ* during the reaction of AO7 with Fenton reagent ($Fe^{II}+H_2O_2$ at pH 4.0).

© 2013 Elsevier B.V. All rights reserved.

1. Introduction

Synthetic dyes are extensively used in textile, leather, paper, pharmaceutical, and food industries, which create ecological and environmental problems [1,2]. Among the synthetic dyes, acid orange 7 (AO7, also named orange II) is extensively used in dyeing industry. AO7 has a relatively simple structure (Table 1) and is commonly used as a model to evaluate technologies to treat dyes [3]. The oxidative treatment technology using a Fenton reagent is preferable over other methods to effectively degrade dyes [4,5]. An appropriate analytical method is needed to evaluate the technology to treat dyes, which not only detects the dye, but also analyzes simultaneously its degradation products in order to learn oxidative pathways.

The traditional methods such as dilution multiple method, paper chromatography, and fluorescence spectrometry cannot detect simultaneously the AO7 and its degradation products. Other commonly used techniques, gas chromatography (GC) and high performance liquid chromatography (HPLC) equipped with mass spectrometry (MS), are able to detect the multiple substances simultaneously with high speed, sensitivity, and efficient selectivity [6,7]. However, these techniques are not appropriate due to high polarity, non-volatility, and thermal instability of AO7 and most of its degradation products [8]. Moreover, these techniques are also not suitable for *in-situ* detection. Furthermore, analyzing target compounds using GC and HPLC techniques in large-scaled wastewater treatment process is prohibited due to high equipment and operating costs.
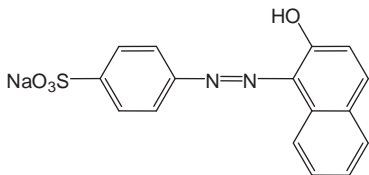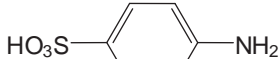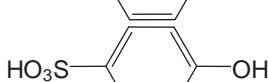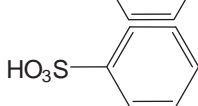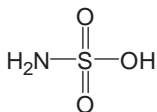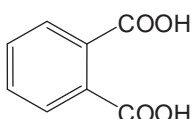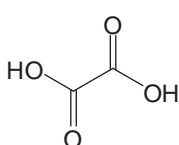
In recent years, the capillary electrophoresis (CE) has demonstrated high efficient separations for polar and ionic substances. CE can be easily coupled with different detectors to analyze variety of molecules [9–12]. Using this technique, promising results have been achieved to separate and to identify dyes in foodstuff, personal care products, textile, and environment and forensic samples [10,13–16]. The known reports on using a CE technique to detect degradation products of dyes are limited to a few works. Takeda et al. [17] used CE–MS and CE–UV detectors to identify AO7 degradation products in wet oxidation process: three kinds of degradation products (4-hydroxybenzene sulfonic acid, phthalic acid and 4-aminobenzene sulfonic acid) were identified. Lu et al. [12] and Zhao et al. [18,19] independently determined the biodegradation products of AO7 by CE–MS; two major degradation

* Corresponding authors at: School of Environmental Science and Engineering, Sun Yat-sen University, Guangzhou 510275, China. Tel.: +86 20 8095 8871; fax: +86 20 3933 2690.
E-mail addresses: cesxya@mail.sysu.edu.cn (Y. Xiong), hechun@mail.sysu.edu.cn (C. He).

Table 1
Linear range, correlation coefficients of calibration curves, and sensitivity of analytes under optimal conditions.

Name	Structural formula	Linear range (μM)	Linearity correlation	Detection limit[a] (μM)
Acid orange 7		0.05–0.82	0.9996	0.037
4-Aminobenzene sulfonic acid		0.10–1.97	0.9991	0.047
4-Hydroxybenzene sulfonic acid		0.05–0.82	0.9997	0.020
Benzenesulfonic acid		0.05–1.02	0.9995	0.027
Sulfamic acid		0.05–0.78	0.9998	0.018
Phthalic acid		0.05–0.91	0.9992	0.035
Oxalic acid		0.02–0.64	0.9992	0.013

[a] The detection limits were calculated based on S/N of 3.

products (benzenesulfonic acid and 4-hydroxybenzene sulfonic acid) were identified. The present study aims to demonstrate simultaneous analysis of six target molecules using a CE technique.

In this paper, capacitively coupled contactless conductivity detector (C^4D) was attached to CE for the analysis of various compounds in complex matrices. To our knowledge, no published literature is known for the determination of degradation products of dyes using a CE-C^4D technique. A CE-C^4D method was therefore first developed to analyze degradation products, which were 4-aminobenzene sulfonic acid [1,20–22], 4-hydroxybenzene sulfonic acid [1,12,17–20,22], benzenesulfonic acid [12,18,22], phthalic acid [7,17,23,24], oxalic acid[1,24], and sulfamic acid. The reaction of AO7 with $^\bullet$OH, generated by the Fenton reagent ($Fe^{II} + H_2O_2 \rightarrow Fe^{III} + {}^\bullet OH + OH^-$), may produce these target molecules. The paper presents separation and identification of degradation products. Based on the analyses, possible pathways for the degradation of AO7 to different degradation products were proposed.

2. Experimental

2.1. Reagents and chemicals

Acid orange 7 (AO7, Color Index No. 15510), benzenesulfonic acid, and sodium 4-hydroxybenzenesulfonate dihydrate were purchased from Aladdin Chemistry Co. Ltd. (Shanghai, China). Sodium oxalate of guaranteed reagent grade was obtained from Tianjin Kermel Chemical Reagent Co., Ltd. (China). Potassium

2-carboxybenzoate and 4-aminobenzenesulfonic acid were bought from Reagent Factory of Shanghai Chemical Reagent Co. Ltd. (China). Sulfamic acid, acetic acid, sodium hydroxide, hydrogen peroxide, nitric acid, and ferrous sulfate were obtained from Guangzhou Chemical Reagent Industries (China). All reagents used throughout the study were of analytical grades unless otherwise stated. Ultrapure water was employed through the study. All stock solutions were kept in a refrigerator at 4 °C. Aliquots of these stock solutions were used to prepare test mixtures. Running buffers were prepared fresh daily by diluting stock solutions.

2.2. Apparatus

The CE-C^4D equipment was composed of a CES2008-C^4D/CD-1B and a CES2008-HV-1B, which was manufactured by School of Chemistry and Chemical Engineering, Sun Yat-sen University, China [25]. The CE instrument control and data collections were performed using an OPTIPLEX 360 personal computer (DELL, USA). The fused-silica capillary was obtained from Hebei Ruifeng Instrumental Co. (China). The dimension of the capillary was 50 μm i.d., 375 μm o.d., 40 cm effective length, and 45 cm total length. The capillary was conditioned by washing it in the following sequence: ultrapure water, 0.1 M HNO₃, ultrapure water, 0.1 M NaOH, and ultrapure water for 5 min each, and finally rinsed with running buffer for 8 min before the first run and for 3 min between each run intervals. During the study, room temperature and humidity were maintained at 25 °C and < 60%, respectively.

2.3. Analysis of degradation products by IC

The final degradation products in the solution after oxidation reactions were determined by Dionex ICS-90 ion chromatography (IC) with an anion column (IonPac AS14A4 × 250 mm). Chromatographic conditions: flow rate (0.80 mL min^{-1}), injection volume (25 μL), column temperature (303 K), eluent (8.0 mmol L^{-1} Na$_2$CO$_3$ + 1.0 mmol L^{-1} NaHCO$_3$), and automatic regeneration suppression system (45 mmol L^{-1} H$_2$SO$_4$).

3. Results and discussion

3.1. Electrophoretic conditions

3.1.1. Selection of running buffer

A baseline signal of CE-C^{4}D results from the running buffer while the detector response signal is essentially the difference in conductance between the analyte ion and the background
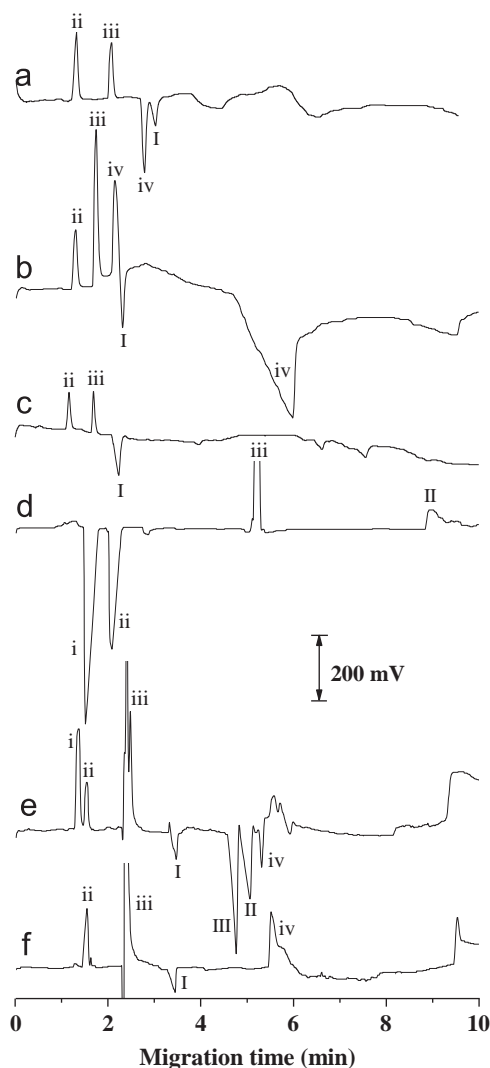

Fig. 1. Electropherograms of test buffers under positive voltage. Test buffer: (a) 2.0 mM EDA, (b) 1.0 mM TEA–0.2 mM SDBS, (c) 0.5 mM H$_3$PO$_4$–1.0 mM TEA, (d) 0.5 mM Cit, (e) 1.0 mM HAc–1.0 mM Tris–4.0 mM TEA, and (f) 0.5 mM HAc–1.0 mM TEA; I: acid orange 7, II: phthalic acid, III: citric acid, i: potassium ion, ii: sodium ion, iii: electroosmotic flow, and iv: system peak. The sample is a mixed solution of AO7 (0.045 mM), benzenesulfonic acid (1.5 mM), phthalic acid (1.5 mM) and citric acid (1.5 mM), which was diluted with running buffer. Conditions: electrokinetic injection: +11 kV × 7 s, and applied voltage: +15 kV.
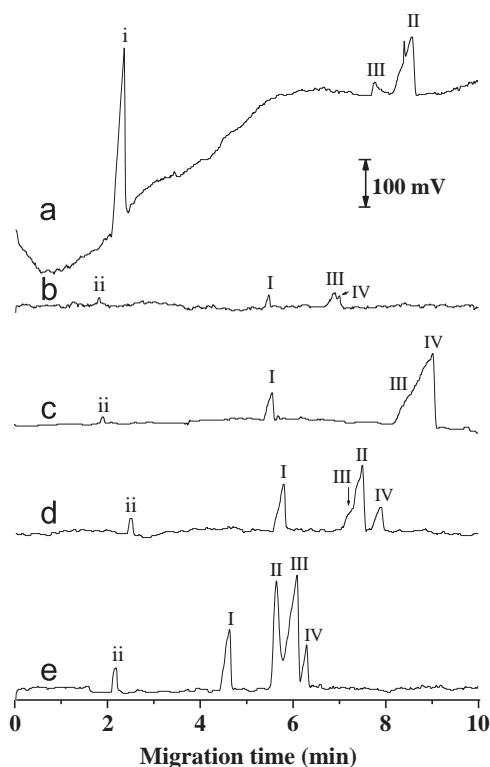

Fig. 2. Electropherograms of test buffers under negative voltage. Test buffer: (a) 0.5 mM Cit, (b) 10.0 mM HAc–1.0 mM Tris, (c) 10.0 mM HAc–0.1 mM NH$_4$Ac, (d) 10.0 mM HAc–0.25 mM TEA, and (e) 10.0 mM HAc; I: 4-hydroxybenzene sulfonic acid (30.0 μM), II: phthalic acid (150.0 μM), III: AO7 (30.0 μM), IV: 4-aminobenzene sulfonic acid (30.0 μM), i: chloride ion, and ii: sulfate ion. The samples are diluted with running buffer. Conditions: electrokinetic injection: −11 kV × 7 s; and applied voltage: −15 kV.

electrolyte [26]. Therefore, an appropriate buffer solution was first selected to obtain high sensitivity and high separability. Several running buffer systems were tested: Na$_2$HPO$_4$–NaOH–CTAB [27], H$_3$PO$_4$–TBAH (tetrabutylammonium hydroxide)–TEA (triethylamine) [16], H$_3$PO$_4$–NaOH [28], Na$_2$HPO$_4$–Tris, Na$_2$HPO$_4$–TEA, H$_3$BO$_3$–Tris–EDTA–Vc–TEPA, H$_3$BO$_3$–Tris–TBAH, Borax–Tris, Borax–NaOH–β-CD [13], NH$_4$Ac–NH$_3$ [19], HAc, HAc–NH$_4$Ac [18], HAc–TEA–β-CD, HAc–TBAH–TEA, HAc–Tris, HAc–Tris–TEA and HAc–Tris–CTAB [25].

Generally, positive ions, electroosmotic flow (EOF), and negative ions show separation when positive voltage is used in capillary zone electrophoresis. The running buffer systems, mentioned above, were thus tested under positive voltage conditions (Fig. 1). It can be seen that satisfactory sensitivity and separability for AO7 and its degradation product could not be obtained. The formed intermediate products of AO7 were mainly organic anions in reaction solution, and the positive voltage may not be favorable to separate the low-pKa anions. The running buffer systems were thus performed under negative voltage conditions. The CE-C^{4}D electropherograms of the target–response systems under negative voltage in citric acid (Cit) and acetic acid (HAc) buffering systems are shown in Fig. 2. Cit had a sloped baseline and no peaks were seen for 4-hydroxybenzene sulfonic acid and 4-aminobenzene sulfonic acid (Fig. 2a). Additions of the baseline regulator (Tris) or the pH regulating agents (NH$_4$Ac, TEA and NaOH) to the HAc had detrimental effects on the sensitivity of peaks (Fig. 2b–d). In the HAc buffer system only, the baseline was relatively stable and the separation for the formed intermediate products of AO7 could be observed (Fig. 2e). Acetic acid was chosen as the running buffer medium for subsequent experiments.

Next, the effect of the running buffer concentration was investigated (Fig. 3). The sensitivity and separability increased with the increase in the concentration of acetic acid buffer from 2.0 to 40.0 mM. All seven compounds were successfully separated using HAc in the concentration range from 18 to 40 mM and the separation degree was greater than 1.5 (Fig. 3d–f). However, 40 mM concentration had relatively large baseline noise (Fig. 3f). Therefore, the acetic acid of 20 mM, which represents the overall combined effect of sensitivity and signal-to-noise ratio, was selected as the optimal buffer concentration for CE separation.

3.1.2. Optimization of separation conditions

The optimal separation conditions of sampling method, injecting voltage and time, and applied voltage were further tested in a simple "one-variable-at-a-time" approach according to the criteria of sensitivity, separability, peak shape, and analysis time. In the acetic acid system, the effect of sample solution matrix on the detection was studied using an electrokinetic injection as the sampling method. The detection sensitivity of ultrapure water matrix was about 10 times higher than that of running buffer matrix. The results were similar to the conditions of field-amplified sample stacking (FASS) [29], which is the simplest on-line concentration technique. The conductance of sample diluted in a solution was much lower than that of background running buffer when the electrokinetic injection was used. The electric field intensity of inlet port was much higher than that in a capillary tube. In this case, the sample ion could be accumulated in the electric field border to achieve an on-column concentration

and electric accumulation effect leading to the enhanced detection sensitivity. Therefore, all samples in the following experiment were injected with the water-dilution method.

The effects of the applied voltage on the electropherograms for the standard compounds are shown in Fig. 4. With the increase in applied voltage from -12 to -19 kV, the migration time shortened and the peaks narrowed. However, it should be noted that the sensitivity decreased and signal-to-noise ratio increased. Considering the injection voltage, the applied voltage of -13 kV was chosen as the optimal CE separation condition (the separation current was around -1.2 μA at -13 kV applied voltage).

The injection time on the separation electropherograms was tested between 4 and 14 s (Fig. 5). Increasing the injection time could lead to an increased amount of sample in capillary to some extent. Hence, the peak height and peak area indexed sensitivity also increased, which are beneficial to the sample detection using a CE-C^{4}D. However, with the increase of sample injection volume, the peak width increased, resulting in a poor peak shape. In addition, the peak height increased slowly or even decreased as the injection time was more than 10 s. Therefore, 10 s was selected as the injection time in order to have an optimal electrophoretic condition.

The effects of injection voltage on the peak height and peak width of electropherograms are shown in Fig. 6. The peak height had a linear relationship to the injection voltage, indicating that higher injection voltage was favorable to the sample detection. However, as mentioned above, higher applied voltage could result in the decrease in the sensitivity and increase in the signal-to-noise ratio. In this case, the injection voltage could not be higher
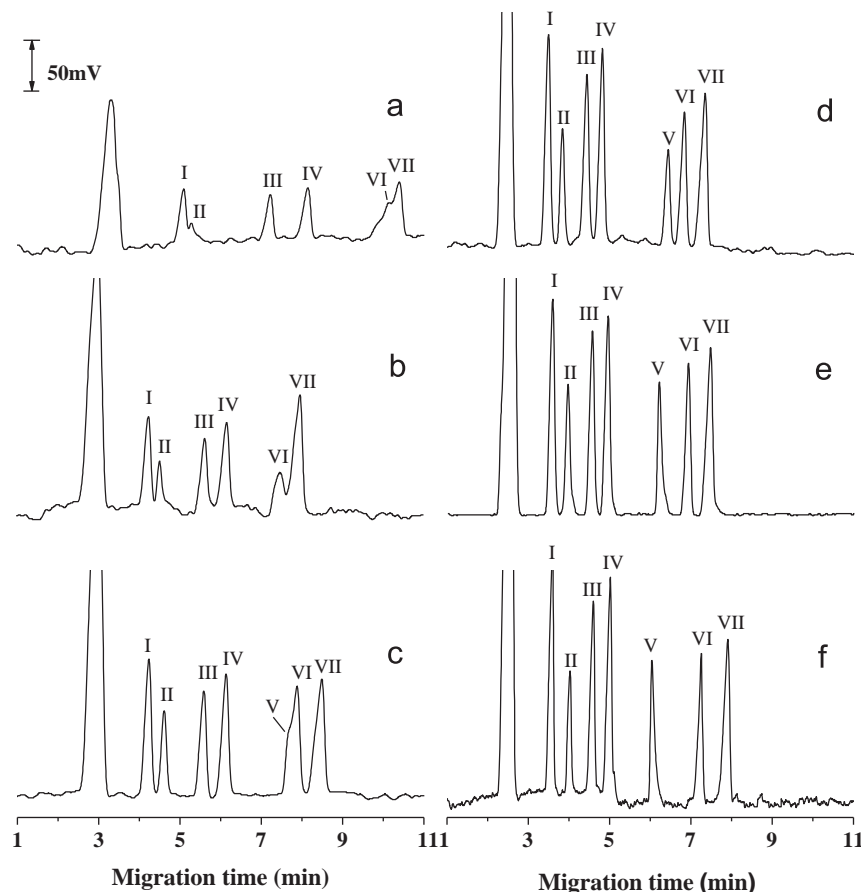

Fig. 3. Effect of acetic acid concentration on electropherogram: (a) 2.0 mM, (b) 4.0 mM, (c) 8.0 mM, (d) 18.0 mM, (e) 20.0 mM, and (f) 40.0 mM; I: sulfamic acid (0.5 μM), II: oxalic acid (0.2 μM), III: benzenesulfonic acid (0.5 μM), IV: 4-hydroxybenzene sulfonic acid (0.5 μM), V: AO7 (0.5 μM), VI: phthalic acid (0.5 μM), and VII: 4-aminobenzene sulfonic acid (1.0 μM). The samples were diluted with ultrapure water. Conditions: electrokinetic injection -12 kV × 10 s and applied voltage -13 kV.
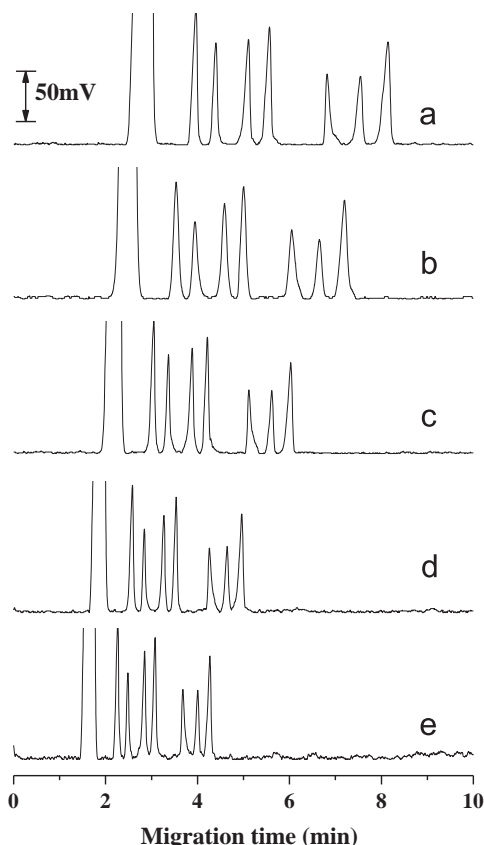
Fig. 4. Effect of applied voltage on electropherogram: (a) −12 kV, (b) −13 kV, (c) −15 kV, (d) −17 kV, and (e) −19 kV. The peak sequence of samples and other conditions were identical to those shown in Fig. 3(e).

Fig. 5. Effect of injection time on peak height and peak width: (a) peak height, and (b) peak width. The peak sequence of samples and other conditions were identical to those shown in Fig. 3(e).

than the applied voltage; thus, the injection voltage and applied voltage were finally selected as −12 kV and −13 kV, respectively. In addition, it could be observed that the average peak width of AO7 increased wavelike with the change in injection voltage from −4 to −14 kV (Fig. 6b). This may be due to the peak tailing characteristic of AO7, which could be verified from the previous electropherograms. Since the commonly used half peak width cannot reflect the peak tailing, the average peak width was selected to reveal the peak pattern in this study.

3.1.3. Quantification

According to the above experimental results, the optimal electrophoretic conditions were as follows: 20 mM acetate acid buffer, electrokinetic injection at 10 s and −12 kV, and −13 kV as applied voltage. The limit of detection, linearity, and correlation coefficient of the seven analytes were tested under the optimized conditions. The results are presented in Table 1. The calibration curves for all analytes were linear in the range from 0.10 to 0.64 μM. Calibration plots with correlation coefficient > 0.999 were obtained by reporting peak areas as a function of analyte concentrations. The detection limits were calculated based on the signal-to-noise ratio of 3. The results indicate that the linearity using CE-C^{4}D method is possible over a wide range of concentration. Therefore, the CE-C^{4}D method can detect these seven analytes with high precision and sensitivity.

3.2. Analysis of degradation products by CE-C^{4}D

The analysis of AO7 degradation products by CE-C^{4}D was carried out in-situ by monitoring the degradation products of
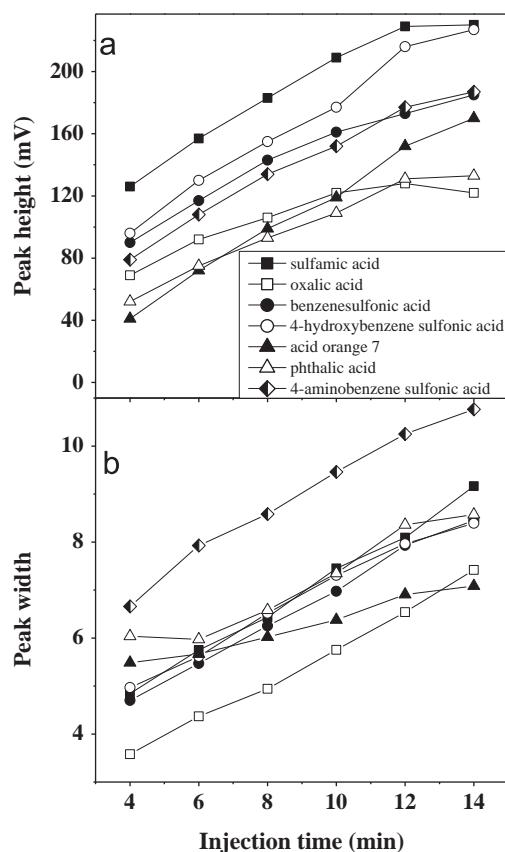

Fig. 6. Effect of injection voltage on peak height and peak width: (a) peak height, and (b) peak width. The peak sequence of samples and other conditions were identical to those shown in Fig. 3(e).
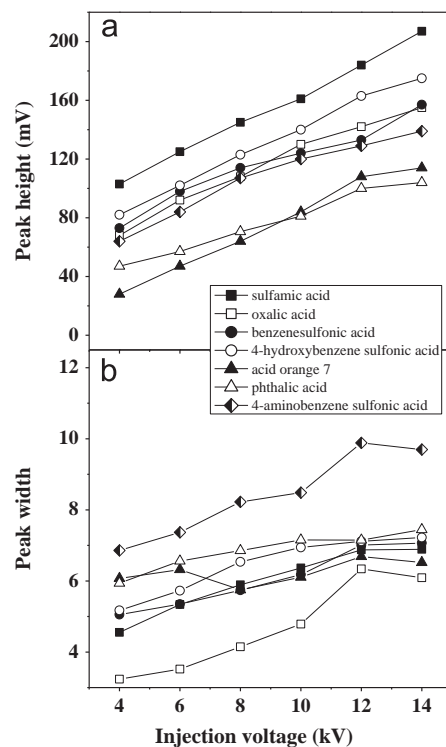
AO7 during its reaction with the Fenton reagent. The identification of compounds in CE-C[4]D electropherogram was carried out both by using the standard-addition approach and by comparing the migration time with standards.

Fig. 7 shows the CE-C[4]D electropherogram of degradation products at different reaction times. Initially, only a small 4-aminobenzene sulfonic acid peak (VII) appeared in the electropherogram. Peaks (V) and sulfate (i) were from AO7 and ferrous sulfate, respectively (Fig. 7a). As reaction progressed, the intensity of the AO7 peak decreased with time (Fig. 7b, c). The intensity of 4-aminobenzene sulfonic acid (VII) peak increased and reached the maximum value at 40 min, followed by decrease with further increase in the reaction time (Fig. 7a–f). Simultaneously, other peaks also appeared, which were identified as sulfamic acid (I), oxalic acid (II), benzenesulfonic acid (III), phthalic acid (VI), and 4-hydroxybenzene sulfonic acid (IV) in turn (Fig. 7b–e). As the reaction time prolonged to 360 min, sulfamic acid (I), phthalic acid (VI), and 4-aminobenzene sulfonic acid (VII) disappeared while benzenesulfonic acid (III) and 4-hydroxybenzene sulfonic acid (IV) peaks decreased (Fig. 7f).

The AO7 degradation products at 50 and 80 min were also analyzed simultaneously using the GC–MS technique. No significant peaks were detected for sulfamic acid (I), oxalic acid (II), benzenesulfonic acid (III), and 4-hydroxybenzene sulfonic acid (IV). Previous studies also demonstrated that oxalate and the compounds with sulfonic groups (e.g. benzenesulfonic acid, 4-hydroxybenzene sulfonic acid and 4-aminobenzene sulfonic acid) were not detectable in GC–MS analysis. Sulfamic acid is not detectable by HPLC or GC–MS techniques because of its instability

and high solubility in water [8,30]. The results indicate that the AO7 oxidized through a number of intermediates prior to its final product, CO_2. Moreover, CE-C[4]D technique is advantageous for in situ detection of AO7 and its degradation products.

The kinetic profiles of AO7 and its major degradation products of AO7 are shown in Fig. 8. AO7 was almost completely degraded
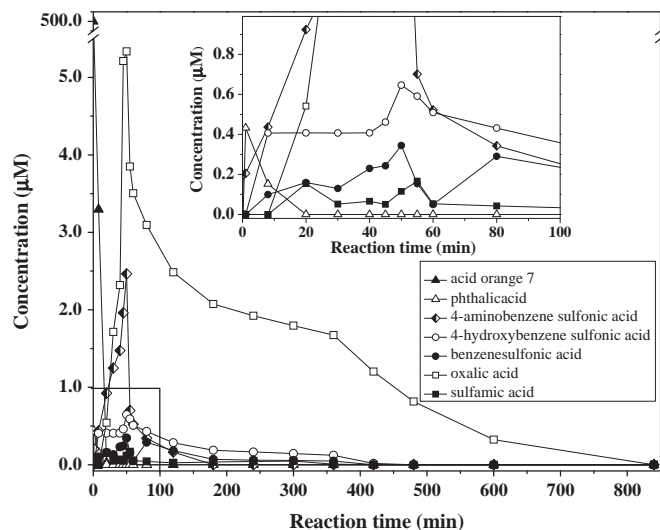

Fig. 8. Kinetic profiles of AO7 and its degradation products in Fenton oxidation reaction at 25 °C. Conditions: 0.5 mM AO7, 0.25 mM Fe^{2+}. The inset is a zoom of rectangular area in Fig. 8.
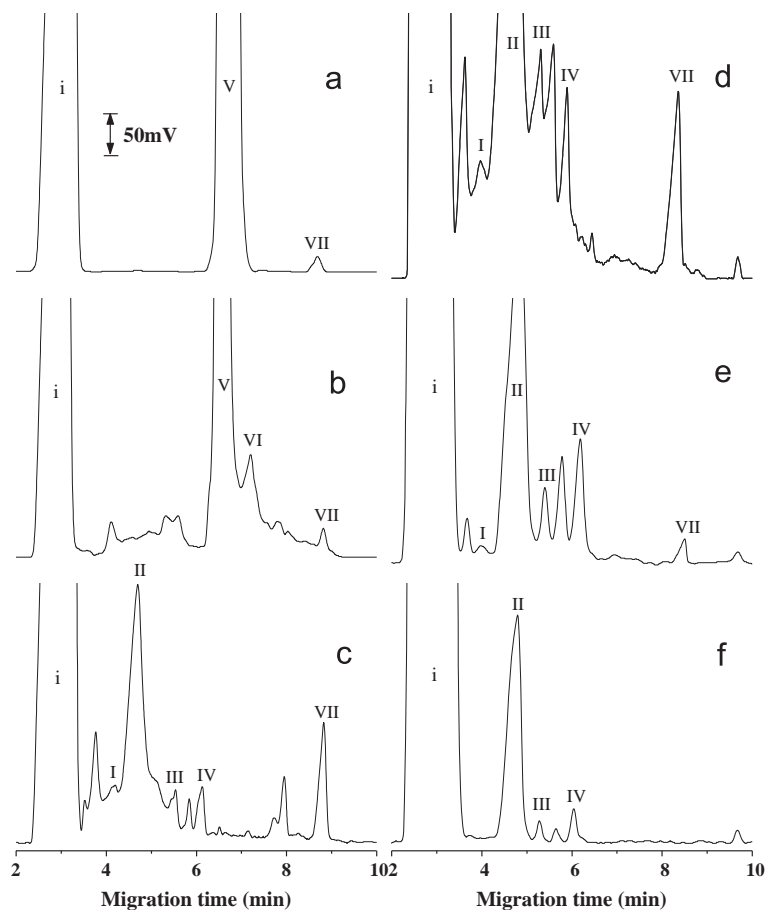

Fig. 7. Electropherogram for separation of real Fenton oxidation samples at different reaction time by CE-C[4]D: (a) 0.2 min, (b) 1 min, (c) 30 min, (d) 50 min, (e) 80 min, and (f) 360 min; I: sulfamic acid, II: oxalic acid, III: benzenesulfonic acid, IV: 4-hydroxybenzene sulfonic acid, V: AO7, VI: phthalic acid, VII: 4-aminobenzene sulfonic acid, and i: sulfate ion. Conditions: 20 mM acetic acid buffer, electrokinetic injection: −12 kV × 10 s; and applied voltage: −13 kV.

in the initial 30 min, while sulfamic acid (I), benzenesulfonic acid (III), 4-hydroxybenzene sulfonic acid (IV), and phthalic acid (VI), increased and reached the maximum concentration in the time period of 50–55 min. Afterward, products decreased rapidly to a lower level after 300 min. In contrast, oxalic acid (II) still remained at a relatively high level, indicating that the oxalic acid (II) degraded at a lower reaction rate. This lower degradation rate may be related to the formation of ferric–oxalate complexes between ferric ions and oxalic acid in the system, which has a slow mineralization rate [22]. Oxalic acid (II) can be mineralized completely by prolonging the reaction time.

3.3. Degradation pathway

Based on the identified products using a CE-C^{4}D technique, possible degradation pathways of AO7 in the Fenton oxidation reaction are proposed (Fig. 9). Initially, the AO7 is broken into two aromatic intermediates, 4-aminobenzene sulfonic acid and 1-amino-2-naphthol, resulting from the cleavage of azo bond

($-N=N-$) [31]. The oxidation of the benzene ring in 4-aminobenzene sulfonic acid leads to the formation of 4-hydroxybenzene sulfonic acid and benzenesulfonic acid. The amino group and sulfonic group detach from these intermediates, generating sulfamic acid, which then rapidly hydrolyzes to sulfate and ammonium ions. Amino-2-naphtol is very unstable and may induce oxidation to yield 1,2-naphthalenediol under aerobic conditions [32,33]. This step is followed by cleavage of 1,2-naphthalenediol to form phthalic acid. Subsequently, the unstable polyhydroxylated may likely form the short-chain carboxylic acids by oxidative ring opening reactions. Oxalic acid is produced through several oxidative steps. Finally, the final product of complete mineralization of oxalic acid is CO_2 [34].

4. Conclusions

In this study, a novel method for simultaneous determination of the degradation products of azo-dyestuff acid orange 7 (AO7) by capillary electrophoresis (CE) with capacitively coupled contactless
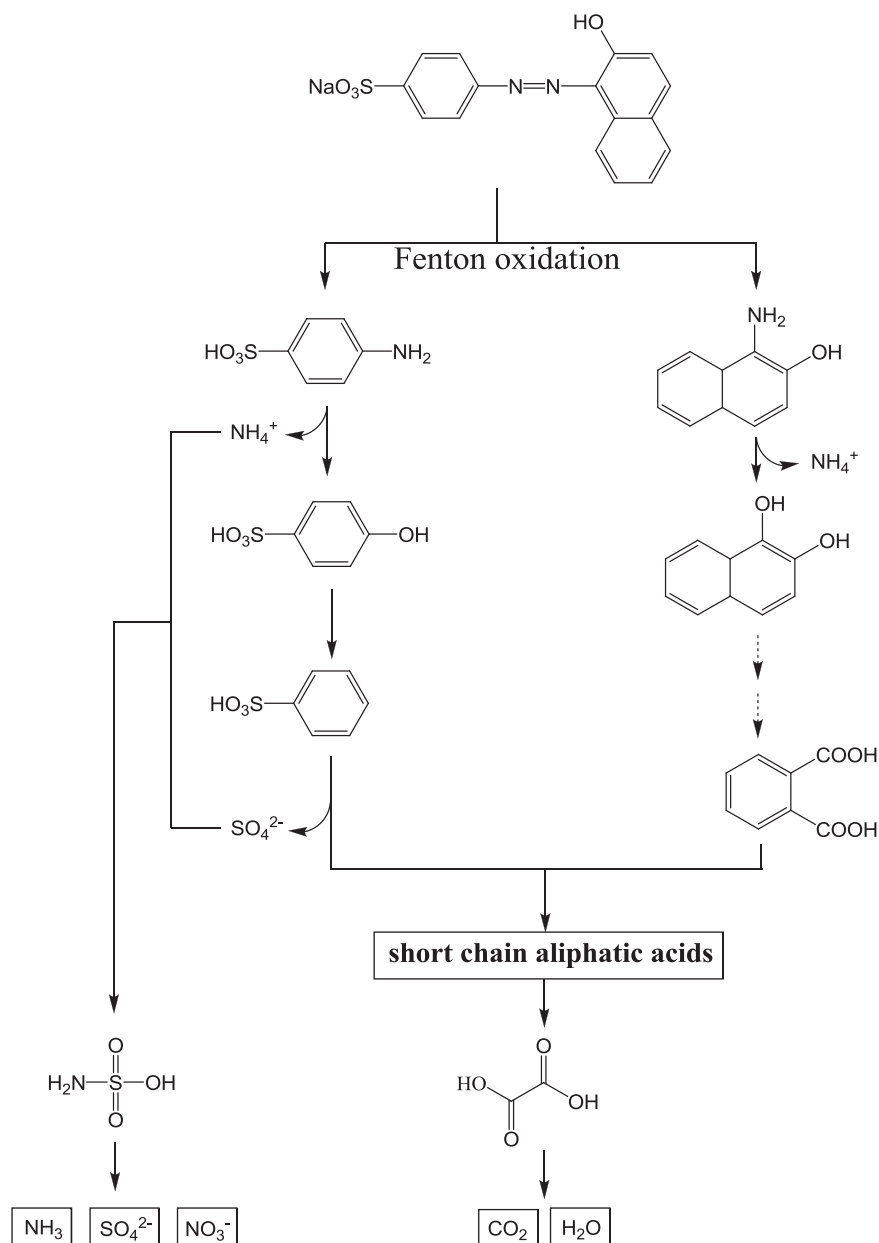
Fig. 9. A possible pathway for degradation of AO7 in Fenton oxidation.

conductivity detection (C^4D) was developed. Optimum conditions were obtained to separate target compounds. Significantly, the separation of the compounds was achievable in 10 min. The developed technique is simple and sensitive for the *in situ* detection of AO7 and its degradation products in oxidation processes. Hence, mechanism of the oxidation of dyes using the CE-C^4D technique can be studied successfully.

Acknowledgments

References

[1] A. Özcan, M.A. Oturan, N. Oturan, Y. Sahin, J. Hazard. Mater. 163 (2009) 1213–1220.
[2] A.K. Verma, R.R. Dash, P. Bhunia, J. Environ. Manage. 93 (2012) 154–168.
[3] A. Mills, C. O'Rourke, V. Kalousek, J. Rathousky, J. Hazard. Mater. 211 (2011) 182–187.
[4] L.L. Zhang, Y.L. Nie, C. Hu, J.H. Qu, Appl. Catal. B: Environ. 125 (2012) 418–424.
[5] N.W. Zhu, L. Gu, H.P. Yuan, Z.Y. Lou, L. Wang, X. Zhang, Water Res. 46 (2012) 3859–3867.
[6] J. Wu, H. Zhang, J. Qiu, J. Hazard. Mater. 215 (2012) 138–145.
[7] L. Xu, H. Zhao, S. Shi, G. Zhang, J. Ni, Dyes Pigm. 77 (2008) 158–164.
[8] X. Chen, W. Wang, H. Xiao, C. Hong, F. Zhu, Y. Yao, Z. Xue, Chem. Eng. J. 193 (2012) 290–295.
[9] D. Arraez Roman, E. Efremov, F. Ariese, A. Segura Carretero, C. Gooijer, Anal. Bioanal. Chem. 382 (2005) 180–185.
[10] A.R. Stefan, C.R. Dockery, A.A. Nieuwland, S.N. Roberson, B.M. Baguley, J.E. Hendrix, S.L. Morgan, Anal. Bioanal. Chem. 394 (2009) 2077–2085.
[11] A.A. Peláez-Cid, S. Blasco-Sancho, F.M. Matysik, Talanta 75 (2008) 1362–1368.
[12] Y. Lu, D.R. Phillips, L. Lu, I.R. Hardin, J. Chromatogr. A 1208 (2008) 223–231.
[13] H.Y. Huang, Y.C. Shih, Y.C. Chen, J. Chromatogr. A 959 (2002) 317–325.
[14] A.V. Jager, F.G. Tonin, M.F.M. Tavares, J. Sep. Sci. 28 (2005) 957–965.
[15] Y. Masukawa, J. Chromatogr. A 1108 (2006) 140–144.
[16] M. Pérez-Urquiza, R. Ferrer, J. Beltrán, J. Chromatogr. A 883 (2000) 277–283.
[17] S. Takeda, Y. Tanaka, Y. Nishimura, M. Yamane, Z. Siroma, S. Wakida, J. Chromatogr. A 853 (1999) 503–509.
[18] X. Zhao, Y. Lu, I. Hardin, Biotechnol. Lett. 27 (2005) 69–72.
[19] X. Zhao, Y. Lu, D.R. Phillips, H.M. Hwang, I.R. Hardin, J. Chromatogr. A 1159 (2007) 217–224.
[20] M. Su, C. He, V.K. Sharma, M.A. Asi, D. Xia, X. Li, H. Deng, Y. Xiong, J. Hazard. Mater. 215 (2011) 138–145.
[21] M.F. Coughlin, B.K. Kinkle, P.L. Bishop, Chemosphere 46 (2002) 11–19.
[22] S. Hammami, N. Bellakhal, N. Oturan, M.A. Oturan, M. Dachraoui, Chemosphere 73 (2008) 678–684.
[23] X. Chen, W. Wang, H. Xiao, C. Hong, F. Zhu, Y. Yao, Z. Xue, Chem. Eng. J. 193 (2012) 290–295.
[24] Y. Peng, D. Fu, R. Liu, F. Zhang, X. Liang, Chemosphere 71 (2008) 990–997.
[25] R. Wei, W. Li, L. Yang, Y. Jiang, T. Xie, Talanta 83 (2011) 1487–1490.
[26] P. Kubáň, P.C. Hauser, Anal. Chim. Acta 607 (2008) 15–29.
[27] A.Z. Carvalho, J.A.F. da Silva, C.L. do Lago, Electrophoresis 24 (2003) 2138–2143.
[28] M. Pérez-Urquiza, J. Beltrán, J. Chromatogr. A 917 (2001) 331–336.
[29] L. Liu, X. Chen, Z. Hu, Microchim. Acta 159 (2007) 125–131.
[30] D. Li, Z. Wang, L. Wang, X. Xu, H. Zhang, Chin. J. Chem. 29 (2011) 147–152.
[31] H.Z. Zhao, Y. Sun, L.N. Xu, J.R. Ni, Chemosphere 78 (2010) 46–51.
[32] A. Troupis, T. Triantis, E. Gkika, A. Hiskia, E. Papaconstantinou, Appl. Catal. B 86 (2009) 98–107.
[33] S.J. Zhang, H.Q. Yu, Q.R. Li, Chemosphere 61 (2005) 1003–1011.
[34] B. Boye, M. Morième Dieng, E. Brillas, J. Electroanal. Chem. 557 (2003) 135–146.